Synthesis, Crystal Structures and Thermal Decomposition Studies of a Series of Copper–Lanthanoid Complexes of 6-Methyl-2-pyridone†

Alexander J. Blake, Vladimir A. Cherepanov, Alister A. Dunlop, Craig M. Grant, Paul E. Y. Milne, Jeremy M. Rawson and Richard E. P. Winpenny*

Department of Chemistry, The University of Edinburgh, West Mains Road, Edinburgh EH9 3JJ, UK

A series of mixed copper–lanthanoid complexes have been synthesised and structurally characterised. All the compounds were made from the reaction of $[Cu_6Na(mhp)_{12}]NO_3$ (mhp is the anion of 6-methyl-2-pyridone) with hydrated lanthanoid nitrates in methanol. In each case X-ray crystallographic analysis revealed a central Cu_2O_2 ring bridged to peripheral lanthanoid (Ln) atoms by mhp ligands. For early lanthanoids (La, Ce and Nd) the complex has a stoichiometry $[Ln_2Cu_2(OMe)_2(mhp)_4(NO_3)_4(Hmhp)_2(MeOH)_4]$, in which the Ln atoms are nine-co-ordinate, with approximate tricapped-trigonal prismatic geometry. For later lanthanoids (Gd, Dy and Yb) the stoichiometry is $[Ln_2Cu_2(OMe)_2(mhp)_4(NO_3)_4(Hmhp)_2(MeOH)_2]$ and the Ln atoms are eight-co-ordinate, with a geometry that can be related to a dodecahedron. For Ln = Sm a disordered co-ordination sphere results, presumably caused by the intermediate ionic radius of Sm leading to very similar stabilities for the eight- and nine-co-ordinate structures. Thermal decomposition studies of these complexes have also been carried out which indicate that decomposition occurs initially to monometallic oxides or oxide carbonates, followed by production of the mixed-oxide phase Ln_2CuO_4 (for Ln = La, Nd, Gd or Dy) or $Ln_2Cu_2O_5$ (for Ln = Er or Yb). In most cases CuO is also found. All oxide and oxide-carbonate phases have been characterised by X-ray powder diffraction.

Several groups have been exploring the synthesis and structures of mixed copper–lanthanoid complexes.[1–8] This work is chiefly motivated by the unusual magnetic interactions found between the d- and f-block elements.[1–4] Our approach has involved using derivatives of the ambidentate bridging ligand 2-pyridone. With the bridging ligand 6-chloro-2-pyridone (Hchp) we have shown that a wide variety of different structures can be accessed through subtle changes in reaction conditions.[6,7] For example, there appears to be a change in the structures seen with large, light lanthanoids such as lanthanum and those with small lanthanoids such as ytterbium.[6] There is also a structural dependency on the solvent in which the reaction is carried out.[7] Here we report synthetic and structural results using the anion of 6-methyl-2-pyridone (mhp) as the bridging ligand; these show a less dramatic dependence of structure on lanthanoid ionic radius. Thermogravimetric studies of the complexes produced have also been carried out, and provide some indication of their usefulness as precursors for the synthesis of mixed-metal oxides.

Experimental

Preparation of Compounds.—The compound $[Cu_6Na(mhp)_{12}]NO_3$ **1** was prepared as described previously.[5] All solvents were used as obtained. Hydrated lanthanoid nitrates were obtained from Johnson Matthey. Elemental analyses for all compounds are given in Table 1.

All reactions followed the same general procedure. Compound **1** (0.29 mmol) was dissolved in dichloromethane (30 cm^3) giving a dark green solution. The hydrated lanthanoid nitrate (1.74 mmol) was dissolved in methanol (10 cm^3) and added to the solution of **1**. The solution became light green and was filtered, then evaporated under reduced pressure to an oil, which was redissolved in methanol (5 cm^3). This was again filtered and allowed to stand. Emerald green crystals formed over a period of 1–5 d. Yields for the reactions are given in Table 1.

Crystallography.—Crystal data and data collection and refinement parameters for compounds **2**–**8** are given in Table 2, atomic coordinates in Tables 3–9 and selected bond lengths in Table 10.

Data collection and processing. Data were collected on a Stoë Stadi-4 four-circle diffractometer equipped with an Oxford Cryosystem low-temperature device[10] operating at 150 K, with graphite-monochromated Mo-Kα radiation and ω–2θ scans using the learnt-profile method.[11] Data were corrected for Lorentz and polarisation factors. Semi-empirical absorption corrections based on azimuthal measurements were applied to data for all compounds except **5**.

Structure analysis and refinement. All structures were solved by Patterson synthesis which revealed the position of the lanthanoid atom. All remaining non-hydrogen atoms were located from subsequent ΔF maps and were refined anisotropically. The hydrogen atoms were included in the refinements at idealised positions (C–H 1.08 Å), and with fixed isotropic thermal parameters [U = 0.06 for **3**, **6**–**8**; U = 0.08 for **2**; U = 0.05 Å^2 for **5**] or with all thermal parameters tied to a common free variable (for **4**). Structure **5** displayed considerable disorder which was manifest in both the bidentate nitrate ions attached to Sm being disordered over two positions. This was modelled by tying all twelve O–N bond lengths to a common value [which refined to 1.276(3) Å]. For one of the half-weight nitrate positions it was also necessary to fix the O···O distances at $\sqrt{3}$ times the free variable to ensure planarity of the nitrate. The site occupancies of the various positions were not refined as the thermal parameters of each position were of comparable magnitude. All calculations used SHELX 76[9] and published scattering factors.[12]

Additional material available from the Cambridge Crystallo-

† *Supplementary data available*: see Instructions for Authors, *J. Chem. Soc., Dalton Trans.*, 1994, Issue 1, pp. xxiii–xxviii.

Table 1 Analytical data for compounds

Compound	Analysis* (%) C	H	N	Yield (%)
2 $[La_2Cu_2(OMe)_2(mhp)_4(NO_3)_4(Hmhp)_2(MeOH)_4]$	33.1 (33.7)	4.2 (4.0)	9.3 (8.8)	25
3 $[Ce_2Cu_2(OMe)_2(mhp)_4(NO_3)_4(Hmhp)_2(MeOH)_4]$	32.4 (33.7)	3.9 (4.0)	9.3 (9.4)	18
4 $[Nd_2Cu_2(OMe)_2(mhp)_4(NO_3)_4(Hmhp)_2(MeOH)_4]$	31.5 (33.5)	4.0 (4.0)	9.3 (8.8)	29
5 $[Sm_2Cu_2(OMe)_2(mhp)_4(NO_3)_4(MeOH)_6]$	28.2 (27.5)	4.0 (4.0)	8.2 (8.0)	32
6 $[Gd_2Cu_2(OMe)_2(mhp)_4(NO_3)_4(Hmhp)_2(MeOH)_2]\cdot 2MeOH$	31.8 (32.9)	3.9 (3.9)	8.8 (9.2)	27
7 $[Dy_2Cu_2(OMe)_2(mhp)_4(NO_3)_4(Hmhp)_2(MeOH)_2]\cdot 2MeOH$	32.3 (32.7)	3.9 (4.0)	9.1 (9.0)	37
8 $[Yb_2Cu_2(OMe)_2(mhp)_4(NO_3)_4(Hmhp)_2(MeOH)_2]$	31.6 (32.1)	3.5 (3.5)	9.2 (9.4)	27
9 $[Er_2Cu_2(OMe)_2(mhp)_4(NO_3)_4(Hmhp)_2(MeOH)_2]\cdot 2MeOH$	31.7 (32.5)	4.1 (3.9)	8.9 (9.0)	37

* Calculated values are given in parentheses.

graphic Data Centre comprises atom coordinates, thermal parameters and remaining bond lengths and angles.

Thermal Decomposition Studies.—Thermogravimetric analyses were carried out on a Stanton Redcroft TG770 instrument at a heating rate of 2 °C min^{-1}. Samples for characterisation by X-ray powder diffraction were prepared by annealing compounds at the required temperature for between 5 and 20 h in a tube furnace. X-Ray powder diffraction studies were carried out using a Phillips PW1730 powder diffractometer, using Cu-Kα radiation (λ 1.5418 Å).

Results and Discussion

Synthesis and Structures.—Reaction of $[Cu_6Na(mhp)_{12}]NO_3$ **1** with hydrated lanthanoid nitrates in a mixture of methanol–dichloromethane (1:1) leads in each case to a green solution. Crystals suitable for X-ray structural analysis can be grown from methanol solution. For all lanthanoids studied the resultant complex contains two copper and two lanthanoid atoms. The only differences observed are in the lanthanoid co-ordination sphere. The structures have a strong resemblance to $[Yb_2Cu_2(OMe)_2(chp)_4(NO_3)_4(MeOH)_4]$ which we reported previously.[6]

For early lanthanoids (Ln) such as La, Ce and Nd, nine-co-ordination is found at the periphery of a molecule of stoichiometry $[Ln_2Cu_2(OMe)_2(mhp)_4(NO_3)_4(Hmhp)_2(MeOH)_4]$ (Ln = La **2**, Ce **3** or Nd **4**), at the centre of which is a Cu_2O_2 ring (Fig. 1). The oxygen atoms in this ring are derived from deprotonated methanol. The copper atoms are each four-co-ordinate, with the remaining two sites occupied by nitrogens from mhp ligands. These ligands bridge to the Ln atoms which are additionally bound to oxygen donors from two bidentate nitrate ions, one protonated pyridone ligand, and two molecules of methanol.

For later lanthanoids such as Gd, Dy and Yb, a similar structure of stoichiometry $[Ln_2Cu_2(OMe)_2(mhp)_4(NO_3)_4(Hmhp)_2(MeOH)_2]$ (Ln = Gd **6**, Dy **7** or Yb **8**) is observed which differs only in the co-ordination number of the Ln atoms which has fallen to eight (Fig. 2). One of the two molecules of methanol attached to the Ln for the lighter lanthanoids has been lost, giving a co-ordination sphere consisting of oxygens from two mhp bridges, two bidentate NO_3^- ions, one Hmhp ligand and one molecule of methanol. This change in co-ordination number is clearly caused by the smaller ionic radii of the heavier f-block metals associated with the lanthanoid contraction.

When the reaction is carried out with hydrated samarium nitrate similar experimental observations are made. Structure solution and refinement is complicated, however, due to disorder in the Sm co-ordination sphere. It appears that Sm, which is of intermediate size, adopts an intermediate structure. The stoichiometry is $[Sm_2Cu_2(OMe)_2(mhp)_4(NO_3)_4(MeOH)_6]$ **5** but both nitrate ions attached to samarium are disordered over two positions. For both nitrates one of the oxygens bound to the Sm atom is common to both fragments. For one of the two nitrates these two sites both involve the nitrate in bidentate co-ordination to Sm [Sm–O distances between 2.515(17) and 2.641(9) Å], but for the second of the two nitrate ions one site involves two oxygen atoms bound to Sm [Sm–O 2.513(9) and 2.381(18) Å] while the second involves one of these oxygens moving away from the samarium to give a weakly bonding contact of 2.756(16) Å. The effect of this is that when the first position is occupied the samarium is nine co-ordinate, bound to two mhp oxygens, two bidentate nitrates and three molecules of MeOH; when the second position is occupied the samarium is closer to eight co-ordinate, bound to two mhp oxygens, one bidentate and one monodentate nitrate and three molecules of MeOH, with one further long bond to a nitrate oxygen.

The Ln–O bond lengths within these compounds also reflect the lanthanoid contraction, becoming shorter on moving from La to Yb (see Table 10). In each case the bond lengths are dependent on the origin of the oxygen donor. The shortest bonds involve mhp and Hmhp ligands, *e.g.* for **4** 2.342–2.364 Å, and the longest bonds involve bidentate nitrate oxygens, *e.g.* for **4** 2.544–2.656 Å. The bonds to methanol ligands are intermediate in length, although closer to the nitrate than the mhp range, *e.g.* for **4** 2.515–2.537 Å (av. e.s.d.s for **4** 0.004 Å). The difference between bond lengths involving methanol oxygens and nitrate oxygens becomes more clear-cut as the lanthanoid atoms become smaller, *e.g.* for **8** the bond range for nitrate oxygens to Yb is 2.418–2.486 Å, while the one Yb–O bond involving a methanol moiety is only 2.302 Å (av. e.s.d.s 0.010 Å).

The co-ordination geometry of the Ln atoms in all these structures is irregular. For the nine-co-ordinate, larger lanthanoids it appears that the best description of the geometry is a distorted tricapped-trigonal prism (Fig. 3). Table 11 lists the angles within the co-ordination polyhedra of **2**–**4**, and also for the co-ordination polyhedron about Sm in **5** which fits best with a tricapped-trigonal prism. Clearly the distortion from a tricapped-trigonal prism is considerable and it appears likely that the chief cause of the distortion is the small bite angle of the

Table 2 Experimental data for the X-ray crystal diffraction studies of compounds **2**–**8**[a]

Compound	**2**	**3**	**4**	**5**	**6**	**7**	**8**
Formula	$C_{42}H_{60}Cu_2La_2N_{10}O_{24}$·4MeOH	$C_{42}H_{60}Cu_2Ce_2N_{10}O_{24}$	$C_{42}H_{60}Cu_2N_{10}Nd_2O_{24}$·4MeOH	$C_{32}H_{54}Cu_2N_8O_{24}Sm_2$·2MeOH	$C_{40}H_{52}Cu_2Gd_2N_{10}O_{22}$·3MeOH	$C_{40}H_{52}Cu_2Dy_2N_{10}O_{22}$·4MeOH	$C_{40}H_{52}Cu_2N_{10}O_{22}Yb_2$·1.5MeOH
M	1621.9	1496.2	1632.6	1426.7	1562.5	1605.0	1541.0
Crystal system	Triclinic	Triclinic	Triclinic	Triclinic	Triclinic	Triclinic	Monoclinic
Space group	$P\bar{1}$	$P\bar{1}$	$P\bar{1}$	$P\bar{1}$	$P\bar{1}$	$P\bar{1}$	$P2_1/c$
a/Å	9.036(5)	9.127(5)	9.011(3)	8.788(6)	9.103(4)	9.130(9)	11.1807(23)
b/Å	11.340(5)	11.503(6)	11.2662(24)	12.153(15)	12.003(4)	12.096(9)	17.136(10)
c/Å	16.062(6)	14.855(7)	16.110(3)	13.913(14)	15.297(6)	15.022(12)	14.771(6)
α/°	85.391(24)	72.59(4)	94.506(18)	114.58(8)	81.155(26)	78.86(4)	90
β/°	85.43(5)	86.47(3)	95.103(23)	101.15(7)	82.886(28)	82.93(8)	93.98(4)
γ/°	88.25(5)	87.99(4)	88.817(17)	92.15(8)	74.789(24)	76.98(6)	90
U/Å^3	1635(1)	1485(1)	1624(1)	1314(1)	1588(1)	1580(1)	2823(1)
Z[b]	1	1	1	1	1	1	2
D_c/g cm^{-3}	1.65	1.67	1.67	1.80	1.63	1.69	1.81
F(000)	818	748	824	712	778	800	1516
Crystal size/mm	1.20 × 0.50 × 0.50	0.80 × 0.23 × 0.22	0.51 × 0.41 × 0.12	0.35 × 0.19 × 0.10	0.27 × 0.19 × 0.14	0.47 × 0.19 × 0.16	0.64 × 0.23 × 0.19
Mounting	Capillary tube	Capillary tube	Oil drop	Fibre	Oil drop	Oil drop	Oil drop
μ/mm^{-1}	2.01	2.32	2.31	3.10	2.81	3.10	4.10
Absorption correction	Semi-empirical	Semi-empirical	Semi-empirical	None	Semi-empirical	Semi-empirical	Semi-empirical
Unique data	3875	3658	4865	3776	4325	4218	3228
Observed data [$I > 2\sigma(I)$]	3399	3018	3020	2618	3639	3861	2698
Max. Δ/σ ratio	0.013	0.007	0.001	0.042	0.046	0.017	0.016
R, R'[c]	0.0588, 0.0763	0.0315, 0.0375	0.0294, 0.0356	0.0420, 0.0588	0.0460, 0.0442	0.0374, 0.0544	0.0550, 0.0741
Weighting scheme, w^{-1}	$\sigma^2(F)+0.000\,50F^2$	$\sigma^2(F)+0.000\,29F^2$	$\sigma^2(F)+0.000\,04F^2$	$\sigma^2(F)+0.0050F^2$	$\sigma^2(F)+0.0040F^2$	$\sigma^2(F)+0.004\,57F^2$	$\sigma^2(F)+0.003\,50F^2$
Goodness of fit	1.030	1.081	0.776	1.541	0.976	1.240	1.110
Largest difference peak/e Å^{-3}	1.52	0.46	0.81	1.69	1.33	1.68	1.42
Measurements of unit cell							
No. of reflections	14	14	25	9	30	22	32
2θ Range/°	28 ⩽ 2θ ⩽ 32	14 ⩽ 2θ ⩽ 32	31 ⩽ 2θ ⩽ 32	17 ⩽ 2θ ⩽ 20	24 ⩽ 2θ ⩽ 26	24 ⩽ 2θ ⩽ 26	28 ⩽ 2θ ⩽ 30

[a] Details in common: T = 150.0(1) K, green tablets, θ range 2.5–22.5°. [b] All molecules lie on inversion centres. [c] Ref. 9.

Table 3 Atomic coordinates for **2** with estimated standard deviations (e.s.d.s) in parentheses

Atom	*x*	*y*	*z*
La	1.079 38(7)	0.203 92(6)	0.267 79(4)
Cu	0.973 35(13)	−0.106 41(11)	0.455 10(8)
N(1R)	0.723 0(10)	0.212 4(9)	0.081 7(6)
O(1R)	0.907 3(10)	0.168 7(8)	0.166 6(5)
C(11R)	0.830 7(14)	0.136 0(12)	0.111 9(7)
C(21R)	0.846 1(14)	0.024 9(12)	0.076 9(8)
C(31R)	0.759 5(15)	0.003 2(14)	0.014 0(9)
C(41R)	0.653 3(16)	0.081 3(16)	−0.014 1(8)
C(51R)	0.634 2(13)	0.189 5(13)	0.021 9(8)
C(61R)	0.520 7(16)	0.283 3(14)	0.001 1(9)
N(2R)	0.797 0(9)	−0.210 7(8)	0.460 6(6)
O(2R)	0.872 2(8)	−0.238 8(7)	0.590 9(5)
C(12R)	0.775 0(12)	−0.260 8(9)	0.539 7(8)
C(22R)	0.647 9(12)	−0.330 3(10)	0.562 6(8)
C(32R)	0.551 6(14)	−0.345 9(12)	0.503 1(10)
C(42R)	0.576 0(15)	−0.295 2(11)	0.422 5(9)
C(52R)	0.703 3(13)	−0.226 5(10)	0.402 0(8)
C(62R)	0.738 2(15)	−0.169 5(12)	0.315 3(8)
N(3R)	1.097 5(10)	−0.185 4(8)	0.369 0(6)
O(3R)	1.059 7(8)	−0.005 7(7)	0.303 7(5)
C(13R)	1.114 3(12)	−0.111 5(9)	0.299 2(8)
C(23R)	1.191 5(14)	−0.151 0(11)	0.225 4(8)
C(33R)	1.246 6(15)	−0.265 5(11)	0.229 2(8)
C(43R)	1.231 3(13)	−0.339 8(11)	0.300 9(8)
C(53R)	1.156 9(12)	−0.296 9(9)	0.370 6(7)
C(63R)	1.136 2(14)	−0.371 0(10)	0.452 7(8)
N(1N)	1.223 1(17)	0.412 4(11)	0.154 5(9)
O(11N)	1.129 8(13)	0.349 4(8)	0.127 6(5)
O(21N)	1.262 7(11)	0.384 1(9)	0.227 3(6)
O(31N)	1.279 2(14)	0.493 4(9)	0.109 6(7)
N(2N)	1.380 3(10)	0.095 1(9)	0.209 6(6)
O(12N)	1.277 6(9)	0.121 7(7)	0.161 0(5)
O(22N)	1.355 8(8)	0.130 6(8)	0.282 9(5)
O(32N)	1.493 6(9)	0.043 5(9)	0.189 3(6)
O(1M)	0.862 8(8)	0.032 2(6)	0.495 8(4)
C(1M)	0.715 1(13)	0.029 1(11)	0.532 1(8)
O(2M)	0.925 5(11)	0.400 3(8)	0.263 9(5)
C(2M)	0.883 8(19)	0.472 8(12)	0.330 2(9)
O(3M)	0.834 7(8)	0.176 5(7)	0.358 2(5)
C(3M)	0.684 4(13)	0.178 3(11)	0.332 6(9)
O(1MS)	0.850 6(14)	0.620 3(10)	0.046 7(7)
C(1MS)	0.971 8(19)	0.673 6(14)	0.075 1(12)
O(2MS)	0.726 1(12)	0.449 4(8)	0.148 1(6)
C(2MS)	0.599 5(19)	0.498 7(19)	0.189 7(14)

Table 4 Atomic coordinates for **3** with e.s.d.s in parentheses

Atom	*x*	*y*	*z*
Ce	0.421 54(4)	0.060 34(3)	0.213 26(3)
Cu	0.532 94(8)	0.131 13(6)	0.480 89(5)
N(1R)	0.796 9(7)	0.251 0(5)	0.008 0(4)
O(1R)	0.602 0(6)	0.182 3(5)	0.105 8(4)
C(11R)	0.677 2(9)	0.271 9(7)	0.060 7(5)
C(21R)	0.650 4(10)	0.393 0(8)	0.058 6(6)
C(31R)	0.741 8(14)	0.483 1(9)	0.003 2(8)
C(41R)	0.859 1(12)	0.455 7(10)	−0.051 0(7)
C(51R)	0.889 1(9)	0.339 4(9)	−0.046 7(5)
C(61R)	1.014 8(11)	0.301 0(10)	−0.096 9(7)
N(2R)	0.711 0(5)	0.213 2(4)	0.502 0(4)
O(2R)	0.638 4(5)	0.103 2(3)	0.650 0(3)
C(12R)	0.736 3(7)	0.174 0(5)	0.596 0(5)
C(22R)	0.859 9(7)	0.212 8(6)	0.628 8(5)
C(32R)	0.955 6(8)	0.287 3(7)	0.564 2(7)
C(42R)	0.928 4(8)	0.326 2(6)	0.468 7(6)
C(52R)	0.807 3(8)	0.287 3(6)	0.439 5(5)
C(62R)	0.769 1(9)	0.325 0(7)	0.337 1(5)
N(3R)	0.415 9(5)	0.279 8(4)	0.424 6(4)
O(3R)	0.448 5(5)	0.196 4(4)	0.304 7(3)
C(13R)	0.396 6(7)	0.288 5(5)	0.332 4(5)
C(23R)	0.326 6(8)	0.391 4(5)	0.274 5(5)
C(33R)	0.276 1(8)	0.481 0(6)	0.310 5(6)
C(43R)	0.295 3(7)	0.470 3(5)	0.405 1(6)
C(53R)	0.364 6(7)	0.369 7(5)	0.460 2(5)
C(63R)	0.389 2(8)	0.350 8(6)	0.562 1(5)
N(1N)	0.255 4(9)	0.014 1(7)	0.051 9(5)
O(11N)	0.367 6(7)	0.079 5(5)	0.034 3(4)
O(21N)	0.217 8(6)	−0.036 9(5)	0.137 0(4)
O(31N)	0.185 5(8)	−0.000 4(6)	−0.012 8(5)
N(2N)	0.133 1(7)	0.202 9(5)	0.191 4(5)
O(22N)	0.151 6(5)	0.113 3(4)	0.263 0(3)
O(12N)	0.241 2(6)	0.233 9(4)	0.131 4(3)
O(32N)	0.017 1(7)	0.260 1(5)	0.179 7(5)
O(1M)	0.633 1(4)	−0.020 4(3)	0.477 5(3)
C(1M)	0.784 3(8)	−0.051 9(6)	0.503 6(5)
O(2M)	0.539 8(6)	−0.116 6(4)	0.156 3(3)
C(2M)	0.514 2(12)	−0.239 1(8)	0.183 6(6)
O(3M)	0.659 6(5)	−0.003 4(4)	0.293 4(3)
C(3M)	0.805 8(9)	−0.011 1(8)	0.258 3(6)

bidentate nitrate ligands. For example, the position of the face-capping oxygen atom is much nearer ideal when the oxygen is derived from a methanol ligand [O(3M)] than when it is part of a nitrate ion. There is also some variation in the degree of distortion between the different complexes, *e.g.* the position of the face-capping methanol oxygen is more nearly ideal in **3** than in either **2** or **4**. The chemical significance of this observation is probably slight, although it may reflect a difference in the intermolecular interactions observed for **3** (see below).

For the eight-co-ordinate, smaller lanthanoids the co-ordination environment is based on a dodecahedron (Fig. 4). Again the geometry is distorted, with the chief distortion being caused by the presence of bidentate ligands. We have chosen to describe the dodecahedron in terms of two perpendicular, intersecting trapezia, and angles relevant to such a description are given in Table 12 for the co-ordination polyhedra in **6–8**. Also included in Table 12 are angles for the co-ordination polyhedron in the disordered structure **5** which fits best with a dodecahedron. As can be seen this description appears markedly less satisfactory for **5** than for **6–8**; this probably reflects the presence of a ninth oxygen donor with a longer contact to Sm (see above).

The copper co-ordination geometry in all the structures is also distorted (Table 13). In each case the geometry observed is intermediate between square planar and tetrahedral, with the angle between the normals to the N–Cu–N and O–Cu–O planes around 40° (*cf.* 0° if square planar or 90° if tetrahedral). There does not appear to be any steric interaction responsible for this degree of distortion. The Cu_2O_2 ring is not an unusual feature, and there are several known examples of methanol being deprotonated to give methoxide bridges between coppers. The Cu–Cu distance of *ca.* 2.96 Å (see Table 10) is similar to that found in other examples, such as $[\{Cu[OC(Bu^t)CHC(O)C_6H_4P(O)Ph_2\text{-}o](OMe)(MeOH)\}_2]$,[13] $[\{HgCu(C_5H_8NO)_2(MeO)(NO_3)\}_2]$[14] or $[Cu_4(C_5H_3ClNO)_4(OMe)_4]$[15] in which the Cu–Cu distances are 2.982(3), 2.957(6) and 2.9664(7) Å respectively.

The crystal packing of **3** is different to that of the other complexes. This is most noticeable in the absence of solvate molecules in the crystal lattice. In the other complexes methanol molecules are located in the lattice, involved in weak hydrogen-bonding interactions with nitrate oxygens or protonated ring nitrogens of Hmhp ligands (O · · · O or O · · · N *ca.* 3.2 Å). In **3** the absence of solvate allows direct hydrogen bonding between neighbouring molecules. The two shortest such interactions are O(31N)–N(1R′) 2.84 and O(2M)–O(11N′) 2.81 Å. The cell dimensions for **3** reflect these differences in crystal packing, with *c* and α markedly different from the values for **2** and **4**.

Thermal Decomposition Studies.—It has been suggested[16] that thermal decomposition of mixed-metal pyridone complexes might provide a useful route to important mixed-metal oxides.

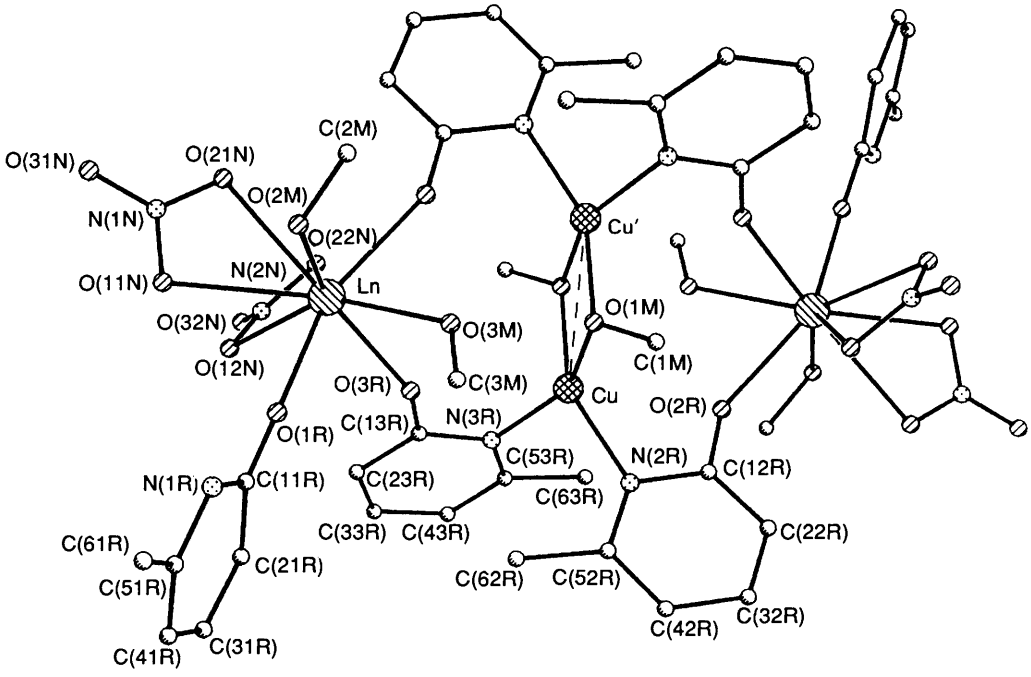

Fig. 1 Structure of $[Ln_2Cu_2(OMe)_2(mhp)_4(NO_3)_4(Hmhp)_2(MeOH)_4]$ (Ln = La **2**, Ce **3** or Nd **4**) complexes showing the crystallographic numbering scheme

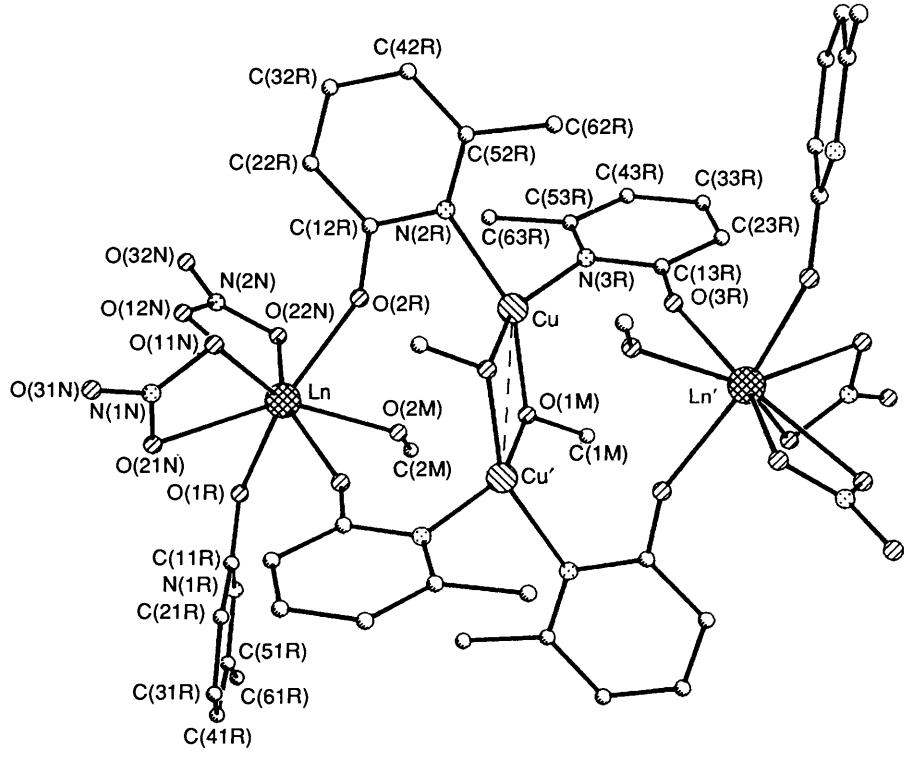

Fig. 2 Structure of $[Ln_2Cu_2(OMe)_2(mhp)_4(NO_3)_4(Hmhp)_2(MeOH)_2]$ (Ln = Gd **6**, Dy **7** or Yb **8**) complexes showing the crystallographic numbering scheme

The evidence supporting this claim, chiefly mass spectroscopy, seemed less than overwhelming. Therefore we have examined in some detail the thermal decomposition of the complexes reported here using thermogravimetric analysis (TGA) and X-ray powder diffraction (XRPD) to characterise the products and the intermediates.

Compounds **2**, **4**, **6**, **8** and a complex which analysed as $[Er_2Cu_2(OMe)_2(mhp)_4(NO_3)_4(Hmhp)_2(MeOH)_2]$ **9** gave similar TGA results. These are summarised in Table 14. Heating the samples up to *ca.* 200 °C leads to weight loss of around 8–10%, consistent with loss of methanol and lattice solvent. The XRPD patterns of samples annealed at this temperature are those of an amorphous solid.

Heating to 250 °C leads to a weight loss corresponding to *ca.* 5% of the original weight, which we believe to be due to loss of the bridging methoxide unit. The XRPD patterns now show distinct peaks for CuO. As the temperature is increased to 350 °C a further 10–14% of the weight is lost, equivalent to loss

Table 5 Atomic coordinates for **4** with e.s.d.s in parentheses

Atom	*x*	*y*	*z*
Nd	1.075 74(3)	0.201 69(2)	1.232 47(2)
Cu	1.026 18(7)	0.107 42(5)	0.956 25(4)
N(1N)	1.220 0(6)	0.408 0(4)	1.344 6(3)
O(11N)	1.121 8(5)	0.344 2(3)	1.371 3(3)
O(21N)	1.256 4(5)	0.377 5(3)	1.270 9(3)
O(31N)	1.273 9(5)	0.492 6(3)	0.387 0(3)
N(2N)	1.373 6(6)	0.097 2(4)	1.290 0(3)
O(12N)	1.269 7(4)	0.121 2(3)	1.339 0(3)
O(22N)	1.346 8(4)	0.130 8(3)	1.216 7(3)
O(32N)	1.487 3(5)	0.045 0(4)	1.312 0(3)
O(1M)	0.863 1(4)	0.031 5(3)	1.004 05(23)
C(1M)	0.713 0(7)	0.029 6(5)	0.967 2(4)
O(2M)	0.834 9(4)	0.175 9(3)	1.142 1(3)
C(2M)	0.683 4(7)	0.172 5(5)	1.167 3(4)
O(3M)	0.929 1(4)	0.396 4(3)	1.234 3(3)
C(3M)	0.887 2(8)	0.468 5(5)	1.167 2(4)
N(1R)	0.726 5(5)	0.213 3(4)	1.416 1(3)
O(1R)	0.905 4(4)	0.166 8(3)	1.329 3(3)
C(11R)	0.830 1(7)	0.135 2(5)	1.386 1(4)
C(21R)	0.845 3(7)	0.025 9(5)	0.421 7(4)
C(31R)	0.759 9(8)	0.001 9(6)	1.484 8(4)
C(41R)	0.653 8(7)	0.086 4(6)	1.513 7(4)
C(51R)	0.636 0(7)	0.189 8(5)	1.477 1(4)
C(61R)	0.520 6(8)	0.284 0(6)	1.497 1(5)
N(2R)	1.201 3(5)	0.213 8(3)	0.965 0(3)
O(2R)	1.121 9(4)	0.239 1(3)	1.094 75(24)
C(12R)	1.224 1(6)	0.262 5(4)	1.045 7(4)
C(22R)	1.348 0(6)	0.331 3(4)	1.070 7(4)
C(32R)	1.448 6(7)	0.350 2(5)	1.013 2(4)
C(42R)	1.423 9(7)	0.300 6(5)	0.930 9(4)
C(52R)	1.300 6(6)	0.232 2(4)	0.908 9(4)
C(62R)	1.265 4(8)	0.175 4(5)	0.821 1(4)
N(3R)	0.902 2(5)	0.185 1(3)	0.867 8(3)
O(3R)	1.055 7(4)	−0.004 2(3)	1.193 53(23)
C(13R)	0.887 9(6)	0.109 7(4)	0.799 5(4)
C(23R)	0.816 0(7)	0.149 1(5)	0.724 3(4)
C(33R)	0.758 5(7)	0.262 9(5)	0.725 3(4)
C(43R)	0.770 0(7)	0.338 1(5)	0.798 1(4)
C(53R)	0.842 3(6)	0.296 9(4)	0.868 9(4)
C(63R)	0.861 0(7)	0.369 5(4)	0.951 8(4)
O(1MS)	0.733 5(5)	0.448 1(3)	1.350 8(3)
C(1MS)	0.604 2(8)	0.501 7(7)	1.309 1(6)
O(2MS)	1.151 7(6)	0.379 2(4)	1.546 0(3)
C(2MS)	1.030 4(9)	0.321 2(6)	0.573 2(5)

Table 6 Atomic coordinates for **5** with e.s.d.s in parentheses

Atom	*x*	*y*	*z*
Sm	0.011 93(9)	0.119 80(6)	0.332 02(5)
Cu	0.031 78(17)	−0.122 26(12)	−0.010 30(10)
O(11N)	0.026 0(11)	0.214 7(8)	0.542 7(6)
N(1A)	−0.102 1(14)	0.257 8(17)	0.527 6(10)
O(21A)	−0.177 3(19)	0.242 2(16)	0.433 7(10)
O(31A)	−0.184 3(20)	0.315 5(15)	0.594 2(13)
N(1B)	−0.065 4(17)	0.293 6(12)	0.541 6(7)
O(21B)	−0.136 5(19)	0.290 7(14)	0.451 2(9)
O(31B)	−0.095 3(19)	0.368 9(12)	0.630 1(10)
O(12N)	−0.150 1(9)	−0.005 7(8)	0.390 2(6)
N(2A)	−0.277 6(12)	−0.047 4(14)	0.317 5(10)
O(22A)	−0.290 1(19)	0.001 2(14)	0.251 3(10)
O(32A)	−0.386 2(16)	−0.119 4(14)	0.318 5(13)
N(2B)	−0.270 4(11)	0.008 9(16)	0.330 8(13)
O(22B)	−0.263 8(21)	0.062 3(16)	0.269 5(12)
O(32B)	−0.401 4(16)	−0.041 6(16)	0.329 2(13)
O(1M)	0.147 8(9)	0.039 2(7)	0.033 5(6)
C(1M)	0.293 2(14)	0.058 0(11)	0.006 7(9)
O(2M)	0.239 7(10)	0.115 4(8)	0.251 0(6)
C(2M)	0.396 0(16)	0.174 5(13)	0.290 5(11)
O(3M)	0.183 1(14)	0.315 6(8)	0.440 5(7)
C(3M)	0.184 8(21)	0.429 8(13)	0.432 0(13)
O(4M)	0.199 7(10)	0.045 2(7)	0.435 3(6)
C(4M)	0.279 2(15)	−0.059 1(12)	0.390 2(10)
O(1R)	−0.070 5(11)	0.204 9(7)	0.214 4(6)
N(1R)	−0.198 9(11)	0.221 4(8)	0.065 6(7)
C(11R)	−0.179 7(14)	0.250 4(10)	0.172 3(9)
C(21R)	−0.278 9(15)	0.323 7(10)	0.230 7(9)
C(31R)	−0.392 1(15)	0.367 9(11)	0.180 9(10)
C(41R)	−0.412 0(14)	0.334 2(11)	0.069 1(11)
C(51R)	−0.312 7(14)	0.261 0(10)	0.013 6(9)
C(61R)	−0.326 4(15)	0.220 0(12)	−0.105 0(10)
O(2R)	0.001 5(9)	−0.070 4(7)	0.190 4(6)
N(2R)	−0.069 9(11)	−0.238 7(8)	0.030 2(7)
C(12R)	−0.057 3(14)	−0.182 6(10)	0.140 6(8)
C(22R)	−0.104 5(14)	−0.258 1(11)	0.190 4(10)
C(32R)	−0.164 0(15)	−0.372 9(11)	0.130 6(10)
C(42R)	−0.182 2(14)	−0.425 9(11)	0.017 8(10)
C(52R)	−0.133 8(14)	−0.356 9(10)	−0.030 4(9)
C(62R)	−0.144 3(17)	−0.407 2(11)	−0.149 8(10)
C(1S)	0.495 4(17)	0.353 5(13)	0.597 3(12)
O(1SA)	0.473(3)	0.302 7(23)	0.656 9(20)
O(1SB)	0.357 3(24)	0.325 9(18)	0.620 0(16)

of NO_3^- ions, presumably in the form of NO_2. At this temperature XRPD shows that $Ln_2O_2(CO_3)$ is being formed in addition to CuO. Heating beyond this temperature, up to around 470 °C (the exact temperature varies between samples, see Table 14) leads to a loss of 34–36% of the weight, presumably due to decomposition of mhp. Further heating leads to a small gradual weight loss which we assign as due to decomposition of oxide carbonates to oxides. Annealing the samples at 900 °C leads to final products which weigh 35.5 ± 1.5% of the substrate. Given the stoichiometry of the starting materials, and the oxides present in the product as identified by XRPD (see below), the calculated weight losses are around 64% which are in very good agreement with the experimental observations.

Although the TGA behaviour of the complexes is similar the XRPD powder patterns of annealed samples vary between the different lanthanoids. In each case peaks due to CuO are found from 200 to 600 °C, and $Ln_2O_2(CO_3)$ phases are also observed in each case at 280–350 °C but the stability and persistence of this oxide carbonate phase varies. XRPD Patterns recorded on samples derived from **2** show that $La_2O_2(CO_3)$ coexists with CuO up to 550 °C before gradually decomposing *via* $La_2O_{2+x}(CO_3)_{1-x}$. This observation agrees with previous studies on the decomposition of lanthanum oxide carbonate.[17] The first peaks which can be unambigiously assigned to La_2CuO_4 are observed in samples annealed at 670 °C.

In samples made by decomposition of **4** and **6** Ln_2CuO_4 phases are found coexisting with $Ln_2O_2(CO_3)$ and CuO at much lower temperatures (*ca.* 280 °C), with peaks due to this phase increasing in intensity as the temperature rises. For **9** $Er_2O_2(CO_3)$ is observed at 280 °C which then decomposes to Er_2O_3 at around 400 °C before finally reacting with CuO to produce peaks for $Er_2Cu_2O_5$ at 600 °C. Finally for **8** peaks due to Yb_2O_3 are observed even at 280 °C, in addition to peaks due to $Yb_2O_2(CO_3)$, and peaks due to $Yb_2Cu_2O_5$ are observed from 520 °C onwards. The final products identified are also different, being a mixture of Ln_2CuO_4 and CuO for Ln = La, Nd or Sm, but being the single phase $Ln_2Cu_2O_5$ for Ln = Er or Yb.

Two further complexes were studied in which the Ln:Cu ratio is different. These complexes, $[Ln_2Cu_4Cl_4(hp)_8(Hhp)_4(H_2O)_4]Cl_2$ (Ln = La or Gd; Hhp = 2-pyridone), were synthesised as described previously.[4] The only significant differences in the behaviour of these compounds was that the fraction of CuO in the final products after decomposition was higher, and also that the Ln_2CuO_4 phase appeared to form at a slightly lower temperature.

It appears from these studies that the decomposition of mixed-metal pyridone complexes proceeds by an initial

Table 7 Atomic coordinates for **6** with e.s.d.s in parentheses

Atom	*x*	*y*	*z*
Gd	0.380 29(3)	0.210 64(2)	0.275 83(2)
Cu	0.411 55(8)	0.092 99(7)	0.553 34(5)
N(1R)	0.754 1(7)	0.232 8(6)	0.054 5(4)
O(1R)	0.555 2(6)	0.230 8(4)	0.157 2(3)
C(11R)	0.644 9(8)	0.181 1(7)	0.095 8(4)
C(21R)	0.636 1(9)	0.076 5(7)	0.066 9(4)
C(31R)	0.738 9(9)	0.032 1(7)	−0.001 4(5)
C(41R)	0.850 8(9)	0.092 6(7)	−0.042 6(5)
C(51R)	0.858 0(8)	0.189 6(7)	−0.013 0(4)
C(61R)	0.974 3(10)	0.256 9(8)	−0.046 3(6)
N(2R)	0.195 5(6)	0.182 0(5)	0.558 8(3)
O(2R)	0.282 0(5)	0.229 5(4)	0.417 7(3)
C(12R)	0.168 8(8)	0.245 3(5)	0.478 7(4)
C(22R)	0.026 2(9)	0.324 6(7)	0.465 3(6)
C(32R)	−0.084 1(10)	0.334 8(9)	0.535 8(7)
C(42R)	−0.054 2(9)	0.269 7(8)	0.618 0(6)
C(52R)	0.084 3(8)	0.191 8(7)	0.626 9(5)
C(62R)	0.122 6(11)	0.114 6(9)	0.712 2(5)
N(3R)	0.477 7(6)	0.170 4(5)	0.639 8(3)
O(3R)	0.527 3(5)	−0.015 2(4)	0.701 2(3)
C(13R)	0.533 3(7)	0.088 8(5)	0.707 4(4)
C(23R)	0.594 5(8)	0.122 2(6)	0.777 1(4)
C(33R)	0.595 8(8)	0.236 6(6)	0.776 4(5)
C(43R)	0.537 1(8)	0.318 8(6)	0.707 4(4)
C(53R)	0.478 4(7)	0.284 8(5)	0.639 8(4)
C(63R)	0.413 5(9)	0.368 7(6)	0.562 1(5)
N(1N)	0.138 5(7)	0.147 7(5)	0.200 2(4)
O(11N)	0.131 2(5)	0.162 6(4)	0.281 1(3)
O(21N)	0.259 1(6)	0.162 0(4)	0.152 6(3)
O(31N)	0.037 9(6)	0.121 6(5)	0.168 7(4)
N(2N)	0.284 8(8)	0.460 9(5)	0.228 4(5)
O(12N)	0.215 6(7)	0.389 3(5)	0.209 5(4)
O(22N)	0.392 1(6)	0.418 4(4)	0.275 4(3)
O(32N)	0.242 1(9)	0.565 0(5)	0.203 0(5)
O(1M)	0.616 7(5)	0.042 0(4)	0.492 2(3)
C(1M)	0.757 5(8)	0.045 3(6)	0.524 1(4)
O(2M)	0.601 8(5)	0.198 1(4)	0.348 9(3)
C(2M)	0.726 0(10)	0.250 8(9)	0.327 4(6)
O(1MS)	0.764 7(10)	0.445 6(7)	0.100 8(7)
C(1MS)	0.895 3(12)	0.456 7(13)	0.151 4(10)
O(9MS)	0.859 7(21)	0.529 1(16)	0.224 8(12)
C(9MS)	0.696(4)	0.562(3)	0.029 7(21)

Table 8 Atomic coordinates for **7** with e.s.d.s in parentheses

Atom	*x*	*y*	*z*
Dy	0.376 92(3)	0.209 47(2)	0.267 23(2)
Cu	0.417 68(8)	0.090 03(6)	0.552 31(5)
N(1R)	0.740 8(6)	0.243 2(5)	0.043 8(3)
O(1R)	0.534 3(5)	0.240 5(4)	0.141 2(3)
C(11R)	0.628 7(7)	0.189 5(5)	0.086 1(4)
C(21R)	0.629 8(8)	0.082 4(6)	0.064 8(5)
C(31R)	0.739 0(9)	0.034 6(7)	0.004 5(5)
C(41R)	0.851 1(9)	0.094 6(7)	−0.038 0(5)
C(51R)	0.853 1(7)	0.195 5(7)	−0.017 9(4)
C(61R)	0.970 2(9)	0.264 3(8)	−0.051 9(6)
N(2R)	0.203 9(5)	0.173 8(4)	0.556 7(3)
O(2R)	0.290 7(4)	0.221 5(3)	0.410 5(3)
C(12R)	0.178 7(7)	0.234 8(5)	0.472 6(4)
C(22R)	0.037 8(8)	0.310 4(7)	0.457 8(5)
C(32R)	−0.068 9(8)	0.319 8(8)	0.528 5(5)
C(42R)	−0.041 3(8)	0.254 9(7)	0.613 5(5)
C(52R)	0.095 9(7)	0.180 7(6)	0.626 8(4)
C(62R)	0.136 7(9)	0.106 8(7)	0.715 6(5)
N(3R)	0.488 3(5)	0.166 9(4)	0.638 8(3)
O(3R)	0.537 3(5)	−0.019 3(3)	0.706 4(3)
C(13R)	0.544 1(6)	0.085 8(5)	0.708 8(4)
C(23R)	0.604 7(7)	0.118 5(5)	0.778 2(4)
C(33R)	0.606 5(7)	0.233 4(5)	0.774 8(4)
C(43R)	0.548 4(7)	0.315 5(5)	0.701 8(4)
C(53R)	0.489 7(7)	0.280 4(5)	0.634 9(4)
C(63R)	0.426 1(9)	0.362 3(6)	0.555 1(5)
O(1MS)	0.741 1(8)	0.462 2(5)	0.066 8(5)
C(1MS)	0.654 0(16)	0.569 4(10)	0.025 8(10)
O(2MS)	0.903 0(7)	0.488 2(6)	0.194 2(5)
C(2MS)	0.848 9(12)	0.559 1(10)	0.263 1(7)
N(1N)	0.133 2(6)	0.146 5(4)	0.195 4(4)
O(11N)	0.130 8(5)	0.153 8(4)	0.279 1(3)
O(21N)	0.249 3(5)	0.167 2(4)	0.145 3(3)
O(31N)	0.029 2(6)	0.119 0(5)	0.165 8(3)
N(2N)	0.275 1(7)	0.457 4(5)	0.234 2(4)
O(12N)	0.198 2(5)	0.387 1(4)	0.217 7(3)
O(22N)	0.399 7(5)	0.413 6(4)	0.265 6(3)
O(32N)	0.225 3(7)	0.561 4(4)	0.218 0(5)
O(1M)	0.617 9(4)	0.045 4(3)	0.488 0(3)
C(1M)	0.760 3(7)	0.050 0(6)	0.518 9(4)
O(2M)	0.602 6(5)	0.196 5(4)	0.333 4(3)
C(2M)	0.720 0(8)	0.260 3(7)	0.311 3(5)

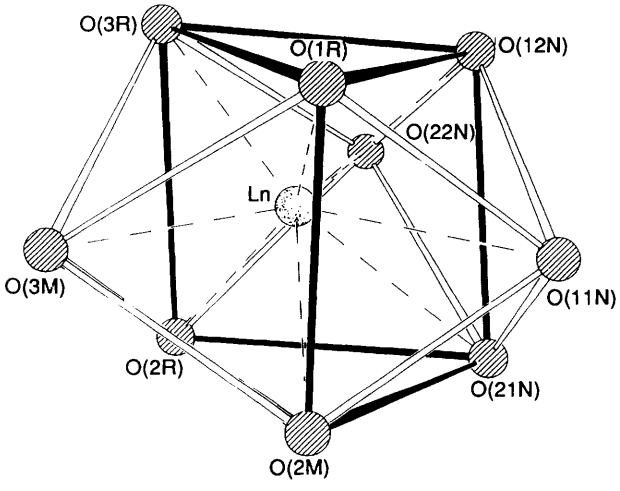

Fig. 3 The co-ordination sphere for the nine-co-ordinate lanthanoid atoms. The trigonal prism is shown with shaded lines, with contacts to face-capping oxygens as open lines

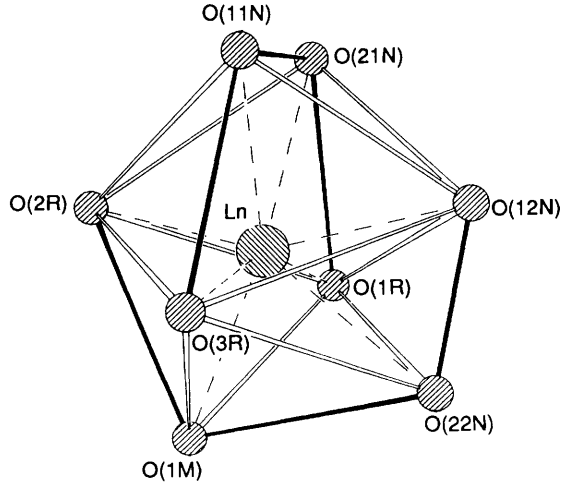

Fig. 4 The co-ordination sphere for the eight-co-ordinate lanthanoid atoms. The two intersecting trapezia referred to in Table 12 are shown with shaded lines, with contacts between oxygens of the differering trapezia as open lines

decomposition to oxide or oxide-carbonate phases of the individual metals. Further heating leads to reaction of these individual phases to give a mixed-metal oxide, plus an excess of the oxide of the metal which was present in excess in the original compound. Thus the decomposition of the mixed-metal complex achieves intimate mixing of the two components. In some cases this intimate mixing leads to the appearance of

XRPD peaks due to the Ln_2CuO_4 phase at comparatively low temperatures, *e.g.* prolonged annealing at 280 °C for **5**. In all cases however at temperatures below 430 °C the mixed oxide is a minor component of the product compared with the homometallic phases.

In a recent report[8] the use of the ambidentate bridging ligand 1,3-bis(dimethylamino)propan-2-ol to prepare heteronuclear copper–lanthanum and copper–yttrium precursors was described. These were in turn decomposed to give uncharacterised oxide phases. Although TGA studies were reported, XRPD was not used to characterise the resultant compounds.[8] The behaviour of these heterometallic precursors appears to be very similar to that reported here for the pyridone complexes, *i.e.* decomposition to a mixture of CuO and the relevant oxide carbonate followed by further reaction to produce a mixed-metal oxide species. The lack of XRPD results in this recent

Table 9 Atomic coordinates for **8** with e.s.d.s in parentheses

Atom	*x*	*y*	*z*
Yb	0.073 73(4)	0.076 13(3)	0.253 28(4)
Cu	−0.125 66(11)	−0.015 78(8)	0.020 58(9)
N(1R)	0.377 3(17)	0.087 3(9)	0.440 4(15)
O(1R)	0.230 9(8)	0.045 4(7)	0.342 3(6)
C(11R)	0.338 0(14)	0.054 2(12)	0.367 9(11)
C(21R)	0.432 3(22)	0.024 3(18)	0.317 6(22)
C(31R)	0.554(3)	0.035(3)	0.349(3)
C(41R)	0.571(3)	0.071 5(21)	0.428(3)
C(51R)	0.498(3)	0.099 4(21)	0.460(3)
C(61R)	0.505(3)	0.139 0(21)	0.545(3)
N(2R)	−0.247 1(8)	0.055 5(6)	0.066 8(7)
O(2R)	−0.097 4(7)	0.054 8(5)	0.176 0(5)
C(12R)	−0.203 0(11)	0.078 2(7)	0.150 8(9)
C(22R)	−0.273 8(12)	0.127 8(11)	0.204 8(10)
C(32R)	−0.385 8(14)	0.147 9(11)	0.168 3(13)
C(42R)	−0.426 9(12)	0.127 5(10)	0.081 4(11)
C(52R)	−0.353 6(11)	0.080 3(8)	0.032 8(10)
C(62R)	−0.390 9(12)	0.052 5(9)	−0.065 6(9)
N(3R)	−0.218 4(7)	−0.115 0(6)	0.012 7(6)
O(3R)	−0.170 6(8)	−0.097 1(5)	−0.131 3(6)
C(13R)	−0.221 9(9)	0.140 1(7)	−0.073 2(8)
C(23R)	−0.273 1(10)	−0.212 8(7)	−0.096 7(9)
C(33R)	−0.317 8(10)	−0.255 7(9)	−0.027 5(11)
C(43R)	−0.314 9(10)	−0.228 1(8)	0.060 4(10)
C(53R)	−0.264 5(9)	−0.157 6(8)	0.079 7(8)
C(63R)	−0.261 0(12)	−0.123 9(9)	0.174 1(8)
N(1N)	0.076 7(11)	0.241 3(8)	0.267 7(8)
O(11N)	−0.005 7(9)	0.206 4(5)	0.219 7(6)
O(21N)	0.161 2(9)	0.199 5(6)	0.301 9(7)
O(31N)	0.073 7(10)	0.312 3(7)	0.273 7(8)
N(2N)	−0.064 6(10)	0.047 9(9)	0.405 0(7)
O(12N)	−0.029 4(9)	0.117 2(7)	0.384 0(6)
O(22N)	−0.032 8(8)	−0.007 0(7)	0.359 7(7)
O(32N)	−0.129 5(10)	0.039 5(8)	0.466 1(8)
O(1M)	0.033 1(7)	−0.067 4(4)	0.032 5(5)
C(1M)	0.051 5(11)	−0.151 7(8)	0.016 1(10)
O(2M)	0.103 9(7)	−0.049 8(5)	0.205 6(6)
C(2M)	0.128 5(14)	−0.120 1(9)	0.253 5(9)
O(1MS)	0.716 9(17)	0.381 8(14)	0.070 6(12)
C(1MS)	0.654(3)	0.310 8(17)	0.067 0(23)

Table 11 Angles (°) within co-ordination polyhedra for Ln complexes with tricapped-trigonal prismatic geometries

Compound	**2**	**3**	**4**	**5***
Range within triangular faces	53.1–64.4	54.7–64.4	53.2–64.5	53.0–63.5
Angle between mean plane of triangular faces	6.2	7.9	5.4	0.6
Range within square faces	81.3–98.4	83.2–100.3	81.1–98.0	83.1–95.1
Angles between mean planes of square faces	59.3, 58.5, 62.2	58.6, 60.5, 60.9	58.3, 59.6, 62.1	54.8, 63.5, 61.2
Range between mean planes of square and triangular faces	79.0–94.7	82.3–94.5	84.7–99.5	87.9–93.7
Angles between normals to square faces and capping atoms				
O(3M)	5.5	2.0	5.4	3.8
O(11N)	15.5	12.7	12.8	12.7
O(22N)	15.8	16.5	15.4	11.2

* The structure is disordered. The polyhedral angles given are for the nine oxygen atoms which give the best tricapped-trigonal prism.

Table 12 Angles (°) within co-ordination polyhedra for Ln complexes with dodecahedral geometries

Compound	**5***	**6**	**7**	**8**
Angles within intersecting trapezia	106.1, 106.8, 117.5, 110.4	113.8, 111.0, 112.8, 102.9	112.0, 112.2, 104.2, 112.6	112.7, 111.3, 111.9, 104.0
Maximum deviation of atom from mean planes of trapezium/Å	0.2931	0.0023	0.0522	0.0639
Angle between mean planes of trapezia	100.1	88.4	89.8	89.8

* The structure is disordered. Angles are given for the oxygen atoms which give the best dodecahedron.

Table 10 Selected bond lengths (Å) for compounds **2**–**8**

Compound	**2**	**3**	**4**	**5**	**6**	**7**	**8**
Ln–O(1R)	2.401(10)	2.393(5)	2.342(4)	2.298(9)	2.289(5)	2.256(4)	2.185(10)
Ln–O(2R)	2.410(8)	2.369(4)	2.364(4)	2.315(8)	2.264(5)	2.219(4)	2.190(8)
Ln–O(3R)	2.409(8)	2.387(4)	2.362(4)	—	2.263(4)	2.230(4)	2.196(9)
Ln–O(11N)	2.699(10)	2.676(6)	2.656(4)	2.641(9)	2.471(5)	2.464(4)	2.441(9)
Ln–O(21N)	2.676(10)	2.675(6)	2.592(4)	2.515(17), 2.634(16)*	2.510(5)	2.476(4)	2.418(10)
Ln–O(12N)	2.585(8)	2.632(5)	2.544(4)	2.513(9)	2.429(6)	2.437(5)	2.421(10)
Ln–O(22N)	2.632(8)	2.595(5)	2.582(4)	2.381(18), 2.756(16)*	2.523(5)	2.520(4)	2.486(10)
Ln–O(2M)	2.588(9)	2.606(5)	2.515(4)	2.472(9)	2.385(5)	2.357(4)	2.302(9)
Ln–O(3M)	2.560(8)	2.522(5)	2.537(4)	2.464(11)	—	—	—
Ln–O(4M)	—	—	—	2.427(9)	—	—	—
Cu–Cu′	2.980(2)	2.974(1)	2.961(2)	2.950(2)	2.971(1)	2.956(2)	2.966(2)
Cu–N(2R)	2.005(9)	1.995(5)	1.990(4)	1.999(10)	1.975(5)	1.986(5)	1.982(10)
Cu–N(3R)	1.965(9)	1.972(5)	1.980(4)	1.970(10)	1.960(6)	1.977(5)	1.990(9)
Cu–O(1M)	1.965(7)	1.953(4)	1.959(4)	1.968(8)	1.970(4)	1.972(4)	1.980(8)
Cu–O(1M′)	1.972(7)	1.962(4)	1.958(4)	1.952(8)	1.947(4)	1.956(4)	1.957(8)

* The atom is disordered over two positions (see text).

Table 13 Bond angles (°) about copper in compounds **2–8**

Compound	2	3	4	5	6	7	8
N(2R)–Cu–N(3R)	97.8(4)	97.32(21)	98.46(17)	96.8(4)	97.09(23)	97.79(20)	100.4(4)
N(2R)–Cu–O(1M)	95.7(3)	96.08(19)	95.59(16)	97.1(4)	153.47(20)	152.49(19)	151.1(4)
N(2R)–Cu–O(1M′)	153.5(3)	153.61(19)	152.28(16)	150.5(4)	97.28(20)	96.16(19)	94.8(4)
N(3R)–Cu–O(1M)	151.8(3)	152.90(19)	150.44(16)	149.2(4)	95.10(21)	95.42(19)	94.8(3)
N(3R)–Cu–O(1M′)	96.5(3)	96.62(19)	96.93(16)	98.4(4)	153.83(21)	152.94(19)	152.4(4)
O(1M)–Cu–O(1M′)	81.6(3)	81.11(17)	81.81(14)	82.4(3)	81.35(18)	82.36(17)	82.3(3)
Angle between N–Cu–N and O–Cu–O planes	37.7	36.6	39.2	42.2	36.2	37.4	37.9

Table 14 Thermogravimetric analysis results for **2**, **4**, **6**, **8** and **9**

Temperature interval/°C	Weight loss (%)	Possible fragments lost
20–(190 ± 10)	8–10	Lattice solvent and MeOH
(190 ± 10)–(250 ± 10)	4–5	MeO^-
(250 ± 10)–(350 ± 10)	10–14	Nitrate NO_3^-
(350 ± 10)–520(**2**,**4**),–470(**6**), –430 (**8**, **9**)	34–36	mhp
550–900	3–5	CO_2 [from $Ln_2O_2(CO_3)$]

report[8] makes it difficult to assess the purity of the resultant phases, however the ratio of metals in the starting materials (La:Cu, 1:2; Y:Cu, 1:3 respectively) suggests that some CuO will remain along with any mixed-metal oxide formed. If such complexes, using either pyridones or other ambidentate bridging ligands, are to be used as precursors for pure mixed-metal oxide phases then this retention of CuO in the final product will continue to present a major problem.

Acknowledgements

We are grateful to the SERC for studentships (to C. M. G. and P. E. Y. M.) and for funding for a diffractometer, the Leverhulme Trust for a post-doctoral fellowship (to J. M. R.), the Royal Society for a visiting fellowship (to V. A. C), the Department of Education for Northern Ireland for a studentship (to A. A. D.). We are also grateful to Dr. G. S. McDougall of the University of Edinburgh for the use of equipment for carrying out the thermal decomposition studies.

References

1 A. Bencini, C. Benelli, A. Caneschi, R. L. Carlin, A. Dei and D. Gatteschi, *J. Am. Chem. Soc.*, 1985, **107**, 8128; A. Bencini, C. Benelli, A. Caneschi, A. Dei and D. Gatteschi, *Inorg. Chem.*, 1986, **25**, 572; C. Benelli, A. Caneschi, D. Gatteschi, O. Giullou and L. Pardi, *Inorg. Chem.*, 1990, **29**, 1751.
2 N. Matsumato, M. Sakamoto, H. Tamaki, H. Okawa and S. Kida, *Chem. Lett.*, 1989, 853.
3 M. Andruh, I. Ramade, E. Codjovi, O. Giullou, O. Kahn and J. C. Trombe, *J. Am. Chem. Soc.*, 1993, **115**, 1822 and refs. therein.
4 A. J. Blake, P. E. Y. Milne, P. Thornton and R. E. P. Winpenny, *Angew. Chem., Int. Ed. Engl.*, 1991, **31**, 1139.
5 A. J. Blake, R. O. Gould, P. E. Y. Milne and R. E. P. Winpenny, *J. Chem. Soc., Chem. Commun.*, 1991, 1453.
6 A. J. Blake, R. O. Gould, P. E. Y. Milne and R. E. P. Winpenny, *J. Chem. Soc., Chem. Commun.*, 1992, 522.
7 A. J. Blake, P. E. Y. Milne and R. E. P. Winpenny, *J. Chem. Soc., Dalton Trans.*, 1993, 3727.
8 S. Wang, Z. Phang, K. D. L. Smith and M. J. Wagner, *J. Chem. Soc., Dalton Trans.*, 1994, 955 and refs. therein.
9 G. M. Sheldrick, SHELX 76, Program for crystal structure refinement, University of Cambridge, 1976.
10 J. Cosier and A. M. Glazer, *J. Appl. Crystallogr.*, 1986, **19**, 105.
11 W. Clegg, *Acta Crystallogr., Sect. A*, 1981, **37**, 22.
12 *International Tables for X-Ray Crystallography*, Kynoch Press, Birmingham, 1974, vol. 4, pp. 19–149.
13 D. A. Wrobleski, J. B. Rauchfuss, A. L. Rheingold and K. A. Lewis, *Inorg. Chem.*, 1984, **23**, 3124.
14 D. M. L. Goodgame, D. J. Williams and R. E. P. Winpenny, *Polyhedron*, 1989, **8**, 873.
15 A. J. Blake, C. M. Grant, P. E. Y. Milne, J. M. Rawson and R. E. P. Winpenny, *J. Chem. Soc., Chem. Commun.*, 1994, 169.
16 S. Wang, S. J. Trepanier and M. J. Wagner, *Inorg. Chem.*, 1993, **32**, 833.
17 V. D. Savin, N. P. Mikhailova and Z. V. Eremenko, *Russ. J. Inorg. Chem.*, 1987, **32**, 1550.

Received 28*th April* 1994; *Paper* 4/02523G